Exact solutions for sonic shocks in van der Waals gases

M. S. Cramer and R. Sen

Citation: Physics of Fluids (1958-1988) **30**, 377 (1987); doi: 10.1063/1.866388
View online: http://dx.doi.org/10.1063/1.866388
View Table of Contents: http://scitation.aip.org/content/aip/journal/pof1/30/2?ver=pdfcov
Published by the AIP Publishing

Exact solutions for sonic shocks in van der Waals gases

M. S. Cramer and R. Sen
Department of Engineering Science and Mechanics, Virginia Polytechnic Institute and State University, Blacksburg, Virginia 24061

(Received 15 August 1986; accepted 28 October 1986)

Exact closed-form solutions for finite amplitude sonic shocks are presented for the case of a van der Waals gas having a constant specific heat. Solutions are provided for both single and double sonic shocks. Sample calculations are presented that include sonic shocks embedded in smooth inviscid flows.

I. INTRODUCTION

A topic of fundamental interest in any area of mechanics and mathematical physics is the nature of shock waves possible in the material of interest. The behavior of single-phase Navier–Stokes fluids is determined by the so-called fundamental derivative[1–6] given by

$$\Gamma \equiv \frac{1}{\rho}\frac{\partial(\rho a)}{\partial \rho}\bigg|_s, \tag{1}$$

where

$$a \equiv \left(\frac{\partial p}{\partial \rho}\bigg|_s\right)^{1/2} \tag{2}$$

is the usual thermodynamic sound speed, ρ is the density, s is the entropy, and $p = p(\rho,s)$ is the pressure. In fluids having $\Gamma > 0$ for all ρ and s the only shock waves possible are compression shocks, i.e., those across which the pressure and density of a fluid particle increases. This is caused by the fact that the shock adiabat, expressed in terms of pressure and specific volume, is necessarily concave upward. The shock adiabat is the locus of thermodynamic states satisfying the Rankine–Hugoniot shock jump relations and is discussed in further detail in the next section. We refer to the case $\Gamma > 0$ as that of positive nonlinearity and note that ideal gases as well as many liquids fall into this category. In the case of negative nonlinearity, i.e., where $\Gamma < 0$, one can show that the only shock waves satisfying the entropy inequality are expansion shocks, i.e., shocks associated with a decrease in pressure and density. A concise proof of these facts is found in Sec. 83–84 of Landau and Lifshitz.[4]

One of the earliest descriptions of negative nonlinearity was given by Bethe,[1] who showed that all fluids having sufficiently large specific heats will possess a region of negative nonlinearity in the general neighborhood of the saturated vapor line. Such an embedded region of negative nonlinearity has been depicted in Fig. 1 for the case of a van der Waals gas. In Fig. 2 the variation of the nondimensional quantity $\rho\,\Gamma/a$ along isentropes is also plotted. In each figure the specific heat at constant volume is taken to be the constant value $c_v/R = 50$, where R is the usual gas constant. An important recent study was performed by Thompson and Lambrakis[7] who employed more accurate equations of state to provide examples of known hydrocarbons and fluorocarbons that are likely to exhibit negative nonlinearity.

Motivation for the study of negative nonlinearity is a result in part of the obvious scientific interest in such inverse behavior. Further interest stems from potential applications. As indicated above, the only shock waves formed when $\Gamma < 0$ are expansion shocks. The fact that expansion shocks carry strong favorable pressure gradients with respect to interactions with boundary layers combined with the large densities, inert character, and excellent heat transfer and phase change properties of the fluorocarbons discussed by previous investigators suggests there may be significant advantages in the use of such fluids in closed-cycle power systems.

It is clear from Figs. 1 and 2 that Γ will change sign in many cases of interest. As a result, the curvature of the shock adiabat may also change sign.[7] This may be seen in Fig. 3 where shock adiabats for a van der Waals gas have been computed and plotted for $c_v/R = 50$. As one expects from a local application of the existence arguments,[4] both compression and expansion shocks may be observed. In fact, both types may occur within the same pulse or wave train.[8–10] This results in a wave evolution that is qualitatively different than the case where Γ does not change sign. A class of shocks

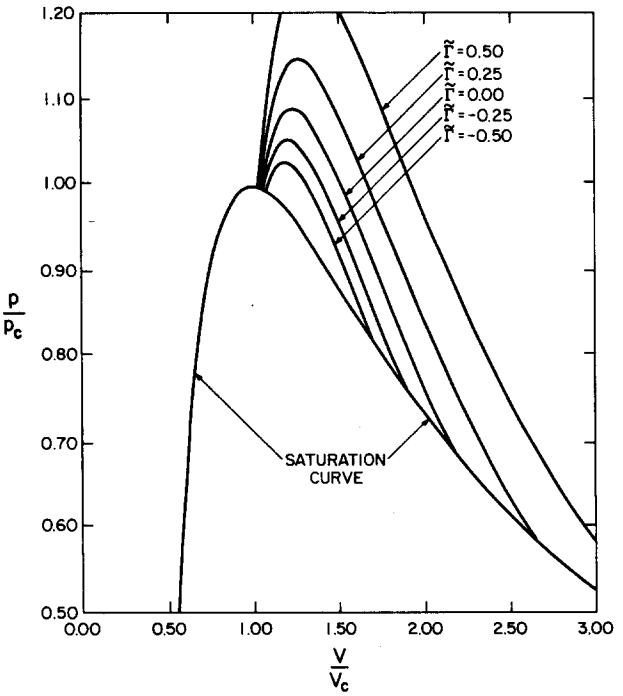

FIG. 1. Constant $\tilde{\Gamma} \equiv \rho\,\Gamma/a$ contours. Van der Waals gas with $c_v/R = 50 = \text{const}$. Subscript c denotes conditions at the thermodynamic critical point.

 0031-9171/87/020377-09$01.90

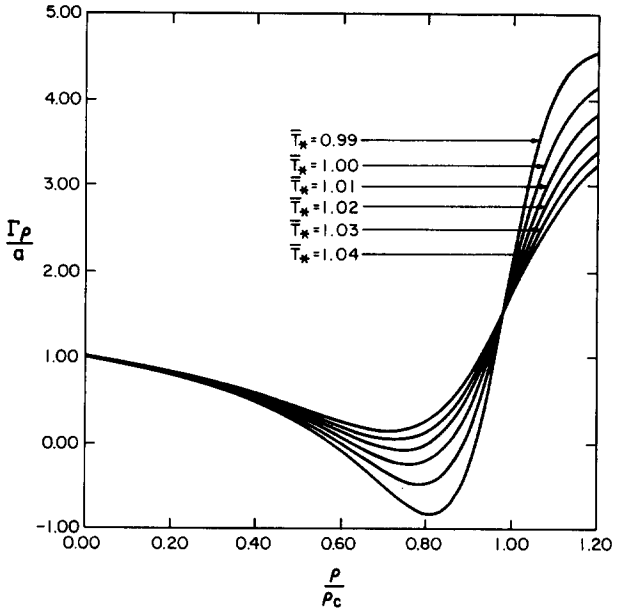

FIG. 2. Variation of $\bar{\Gamma}\equiv\rho\,\Gamma/a$ along isentropes. Gas model is the same as in Fig. 1. The parameter $\bar{T}_*$ is a reference temperature such that each isentrope goes through the point $V=2V_c$, $T=\bar{T}_*T_c$, where T denotes the absolute temperature.

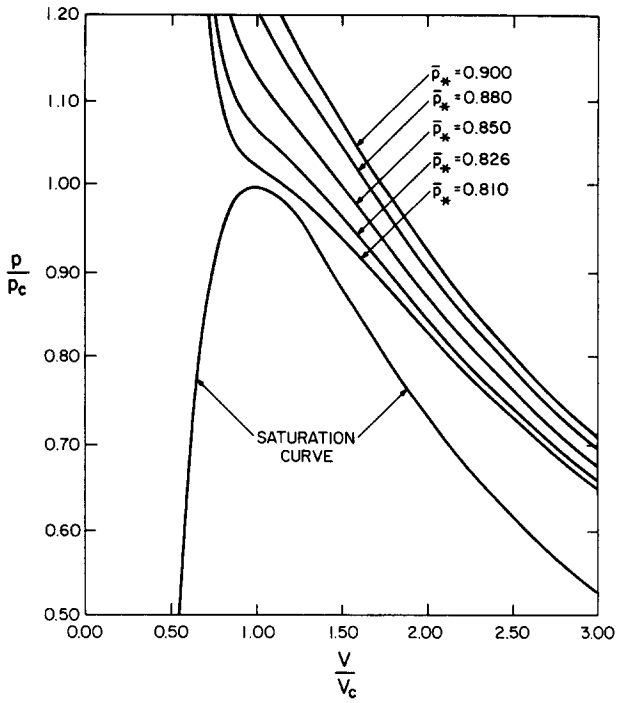

FIG. 3. Computed shock adiabats for a van der Waals gas with $c_v/R=50=\text{const}$. Each adiabat goes through the point $V=2.1V_c$, $p=\bar{p}_*p_c$.

not possible when Γ is strictly positive or strictly negative are sonic shocks. Sonic shocks have a speed identical to either the upstream or downstream convected sound speed. That is, the Mach number relative to the shock is identically one. Thompson and Lambrakis[7] have pointed out that double sonic shocks are also possible; in this case both Mach numbers are 1. While it is clear that sonic shocks are analogous to the Chapman–Jouquet shocks of detonation and deflagration wave theory, it should be pointed out that the shock waves of the present study occur in nonreacting flows and are therefore the result of fundamentally different physical processes.

Previous investigations[7–9] have shown that sonic shocks are closely associated with the partial disintegration of both compression and expansion shocks. These studies as well as the discussion of the next section indicate that sonic shocks will frequently be the shock of maximum strength in many flows of interest. Furthermore, Cramer and Kluwick[8] have analyzed the structure of weak shocks in which the sign of Γ changes across the shock. There it was shown that sonic shocks approach the inviscid conditions algebraically rather than exponentially. Thus, sonic shocks are not only new and interesting phenomena in the inviscid theory but have a fundamentally different dissipative structure. The calculation of this dissipative structure will require accurate estimates of the upstream and downstream states; the need for this accuracy has provided an additional motivation for the present study.

For sufficiently simple equations of state exact solutions for nonsonic shocks are easily obtained. However, the authors know of no closed-form solutions for sonic shocks. It appears that previous authors have relied on graphical or approximate means for the computation of these shocks. Thus, even the simplest flow problem will involve the complications and error inherent in the particular approximation scheme used. Double sonic shocks are likely to be even more difficult because we need to find two double roots of a polynomial simultaneously. The contribution of the present study is to provide exact closed-form solutions for sonic shocks in van der Waals gases with a constant c_v. Thus, many important flows may be computed exactly. Questions of convergence and uniqueness are essentially eliminated; this is particularly important in an area where many results are new and qualitatively different from those of the perfect gas theory. These results are also expected to simplify more complicated problems by minimizing the calculations and approximations needed. It is likely that numerical schemes will be necessary to compute sonic as well as nonsonic shocks when highly accurate and specialized equations of state are employed. The exact solutions established here will also be useful as a check on these general schemes. Because of the importance and prevalence of sonic shocks in problems involving mixed nonlinearity, the present results are of considerable practical and theoretical interest and we expect to see both long and short term benefits arising from the development of these exact solutions.

In the next section we give background material necessary for the general study of shock waves in any fluid that possesses an embedded region of negative nonlinearity. Most of Sec. II should be regarded as a review and application of the known results found in many texts.[4,6] In Sec. III we present the exact solutions for both single and double sonic shocks as well as the formulas needed for the computation of the pressure, temperature, entropy jumps, and the upstream and downstream Mach numbers. In Sec. IV we show how these formulas may be combined with the method of charac-

teristics to give examples of finite amplitude sonic shocks embedded in smooth flows. The cases chosen are the important but simple flows generated by step function initial conditions. An advantage of this choice is that the whole flow field may be computed with a minimum of numerical approximation. These flows may also be recognized as those generated by an impulsive piston motion and as portions of the flow generated in a shock tube. With some modification, the initial stages of the evolution of a finite amplitude square wave may be described as well as some of the simpler cases of the reflection of shock waves from end walls; these flows will be addressed in a more complete fashion in future studies.

II. GENERAL CONSIDERATIONS

The Rankine–Hugoniot conditions for any fluid are

$$[w\rho\,] = 0, \tag{3}$$

$$w_1 w_2 = [p]/[\rho\,], \tag{4}$$

$$[h] = \tfrac{1}{2}((\rho_2+\rho_1)/\rho_2\rho_1)[p], \tag{5}$$

where h is the fluid enthalpy and w denotes the normal component of the relative velocity between the fluid and the shock. The subscripts 1 and 2 denote conditions before and after the shock relative to a fluid particle and the brackets denote the jump in the indicated quantity, i.e., $[Q] = Q_2 - Q_1$, where Q is any quantity. Equations (3)–(5) are recognized as the mass, momentum, and energy equations; the latter is usually referred to as the Hugoniot relation. In addition to the jump conditions (3)–(5), admissible shock waves must satisfy the entropy inequality

$$[s] \geqslant 0 \tag{6}$$

and the stability condition

$$M_1 \geqslant 1 \geqslant M_2 > 0. \tag{7}$$

Here s is the entropy,

$$M_i \equiv w_i/a_i, \quad i = 1,2, \tag{8}$$

are the upstream and downstream Mach numbers, and a is the sound speed (2). Condition (7) states the well-known requirement that the flow upstream of a shock must be supersonic and that the downstream flow must be subsonic. This is equivalent to the speed ordering relation discussed in Refs. 7, 8, 9, and 11.

The Hugoniot equation (5) gives the locus of thermodynamic states accessible through a shock wave. That is, it yields a relation

$$\phi(p_1, \rho_1, p_2, \rho_2) = 0.$$

In the last section we referred to this as the shock adiabat.

The curvature of the shock adiabat plays a key role in the determination of admissible shocks. For the fluids of interest here it may be shown that the speed-ordering relation (7) may be replaced by the slope-ordering condition

$$\left.\frac{dp}{dV}\right|_2 \leqslant \frac{[p]}{[V]} \leqslant \left.\frac{dp}{dV}\right|_1, \tag{9}$$

where $V = \rho^{-1}$ is the specific volume. The derivatives denote the slopes of the shock adiabat evaluated at upstream and downstream conditions. The geometrical interpretation of $[p]/[V]$ is the slope of the chord connecting the upstream and downstream states. The equalities in (9) correspond to sonic conditions at the indicated side of the shock. Thus, if a shock is sonic on the downstream side, $M_2 = 1$ and

$$\frac{[p]}{[V]} = \left.\frac{dp}{dV}\right|_2.$$

The chord connecting upstream and downstream states of a sonic shock will therefore be tangent to the shock adiabat at the sonic side. Furthermore, it should be clear that sonic shocks are only possible when the curvature of the shock adiabat changes sign.

In Fig. 4 we have sketched a shock adiabat typical of fluids having embedded regions of negative nonlinearity, see also Fig. 3, along with various sonic and nonsonic shocks.

The discussion presented so far deals primarily with the stability condition (7). When the shock adiabat is strictly concave upward or strictly concave downward the stability condition and entropy inequality are equivalent. However, for the mixed nonlinearity discussed here, any one or even two of the three conditions (6) and (7) may be violated while the remaining conditions are satisfied. An example where the speed-ordering condition has been violated with an increase in entropy is represented by C1–C3 in Fig. 4(a). We have also found examples of shocks which satisfy the speed-ordering conditions (7) but violate the entropy inequality (6). For the van der Waals gas with a constant nondimensional specific heat given by $c_v/R = 50$, we find that one such shock is given by

$$\bar{\rho}_1 = 0.45, \quad \bar{p}_1 = 0.8, \quad M_1 \approx 1.02, \quad \bar{\rho}_2 \approx 1.02,$$
$$\bar{p}_2 \approx 1.08, \quad M_2 \approx 0.94, \quad [s]/c_v = -2.8\times 10^{-3}.$$

In all that follows, the overbars will denote quantities scaled with values at the thermodynamic critical point.

III. EXACT SOLUTION

The equation of state of a van der Waals gas is

$$p = RT/(V-b) - \alpha/V^2, \tag{10}$$

where T is the absolute temperature and R is the usual gas constant. The parameters α and b are positive constants that account for the intermolecular forces and molecule size. In terms of these parameters the pressure, specific volume, and temperature at the thermodynamic critical point are given by

$$p_c = \alpha/27b^2, \quad V_c = 3b, \quad RT_c = 8\alpha/27b. \tag{11}$$

The specific heat at constant volume c_v will be taken to be a constant and large enough to result in the region of negative nonlinearity depicted in Figs. 1 and 2; Bethe[1] and Thompson and Lambrakis[7] have provided estimates for the minimum value of c_v required for van der Waals gases.

For this gas model the appropriate expression for the enthalpy h is

$$h = c_v T - \alpha\rho + p/\rho + \text{const.}$$

When this expression and (10) are substituted in the Hugoniot equation (5), we find that the shock adiabat for a van der

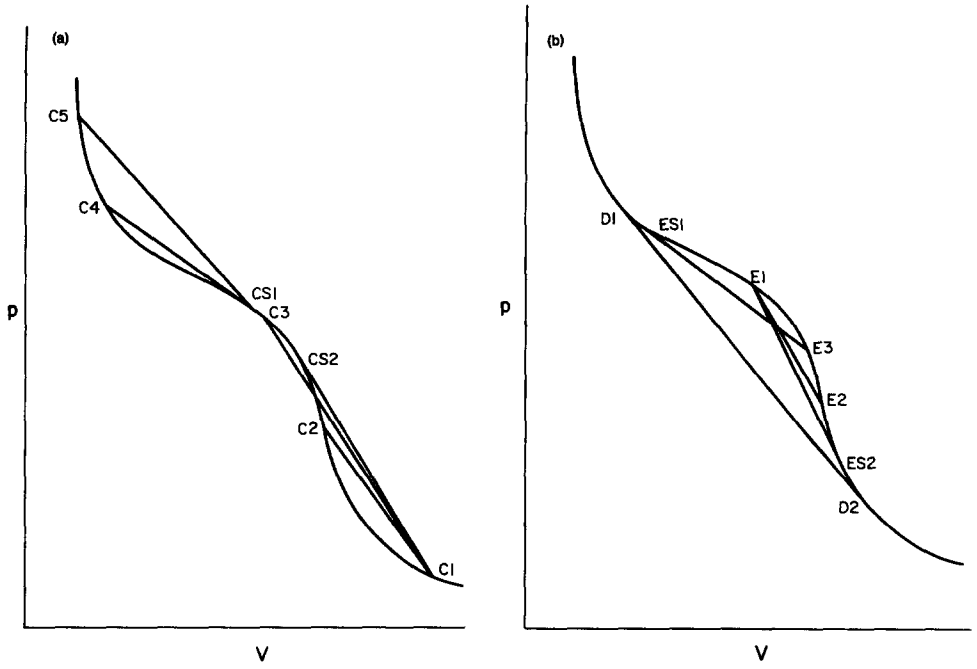

FIG. 4. (a) Examples of compression shocks. C1–C2 and CS1–C5 are nonsonic compression shocks satisfying (6)–(7). CS1–C4 has upstream sonic conditions, $M_1 = 1$, $M_2 < 1$, and C1–CS2 has downstream sonic conditions $M_1 > 1$, $M_2 = 1$. C1–C3 has $M_1 > 1$, $M_2 > 1$ and is therefore inadmissible. In all cases the entropy inequality (6) is satisfied. (b) Examples of expansion shocks. E1–E2 is a nonsonic expansion shock satisfying (6)–(7). E1–ES2 has downstream sonic conditions with $M_1 > 1$, $M_2 = 1$. ES1–E3 has upstream sonic conditions with $M_1 = 1$, $M_2 < 1$. D1–D2 illustrates the double sonic shock $M_1 = M_2 = 1$. In each case (6) is satisfied.

Waals gas may be written

$$A = \frac{3\bar{p}_i(1+\delta) + (9/\overline{V}_i^2\zeta_i)(\delta - 1 + (1+\zeta_i)/3\overline{V}_i\zeta_i)}{3\overline{V}_i\zeta_i((2+\delta)/2) - 1 - \frac{3}{2}\delta\overline{V}_i}, \tag{12}$$

where $i = 1,2$, $\delta \equiv R/c_v$, and

$$[\bar{p}]/[\overline{V}] = -A, \tag{13}$$

$$\zeta_1 \equiv \overline{V}_2/\overline{V}_1, \tag{14}$$

$$\zeta_2 \equiv \overline{V}_1/\overline{V}_2. \tag{15}$$

This form of the shock adiabat is seen to be equivalent to that given by Thompson and Lambrakis.[7] The choice $i = 1$ yields an explicit expression for the downstream pressure $\bar{p}_2$ as a function of $\bar{p}_1$, $\overline{V}_1$, and $\zeta_1 = \overline{V}_2/\overline{V}_1$. The choice $i = 2$ yields the upstream pressure $\bar{p}_1$ provided the downstream conditions $\bar{p}_2$, $\overline{V}_2$ and shock strength $\zeta_2 = \overline{V}_1/\overline{V}_2$ are known. The shock adiabats in Fig. 3 were computed from (12)–(15) with $\delta = 0.02$.

Once the thermodynamic state on each side of the shock is determined, the Mach numbers (8) may be obtained through use of the mass and momentum equations (3)–(4) and definition of A (13). These are found to be

$$M_i = (\overline{V}_i/3\bar{a}_i)A^{1/2}, \tag{16}$$

where, for a van der Waals gas with constant c_v,

$$\bar{a}_i = \left(\frac{2}{3}\right)^{1/2}\left(\frac{4\overline{T}_i\overline{V}_i^2(1+\delta)}{(3\overline{V}_i - 1)^2} - \frac{1}{\overline{V}_i}\right)^{1/2}. \tag{17}$$

Here

$$\overline{T}_i = ((3\overline{V}_i - 1)/8)\,(\bar{p}_i + 3/\overline{V}_i^2) \tag{18}$$

is the absolute temperature scaled with its value at the critical point. Equation (18) is also seen to be the nondimensional version of the equation of state (10). We may also recognize (17) as a nondimensional version of the thermodynamic sound speed for a van der Waals gas where dimensional and nondimensional values are related by

$$a = (\alpha/b)^{1/2}\bar{a}. \tag{19}$$

The entropy jump may be also computed once the upstream and downstream states are known; the expression for this will be given later.

The determination of exact solutions for sonic shocks requires that we fix the Mach number at 1 and solve (12)–(18) for the shock strength, e.g., ζ_i. In general the adiabat (12) may be rearranged to form a cubic equation for ζ_i,

$$E_i\zeta_i^3 - F_i\zeta_i^2 - G_i\zeta_i - 3/\overline{V}_i^3 = 0, \tag{20}$$

where

$$E_i = 3A\,((2+\delta)/2)\overline{V}_i,$$

$$F_i = (1 + 3\delta\overline{V}_i/2)A + 3\bar{p}_i(1+\delta),$$

$$G_i = 9((\delta - 1)/\overline{V}_i^2) + 3/\overline{V}_i^3.$$

Equation (20) has either one or three real roots; these roots are illustrated in Fig. 5. The shock 7-3 is typical of cases having only one real root and the shock 6-5-4-3 is typical of those having three real roots. A sonic shock is a double root of (20). This is represented in Fig. 5 by the chord 1-2-3 tangent, i.e., sonic, at 1. Here we have held the downstream point 3 fixed and rotated the chord until points 5 and 6 collapse to the sonic point 1. The double sonic shock D1–D2 is recognized as the case where the remaining roots are also double roots.

If we now set $M_i = 1$, we find that the cubic (20) has roots

$$\epsilon_i = 0,$$

$$\epsilon_i = (B_i - 3)/2 \pm \{((B_i - 3)/2)^2 - 3 + 2B_i + C_i\}^{1/2}, \tag{21}$$

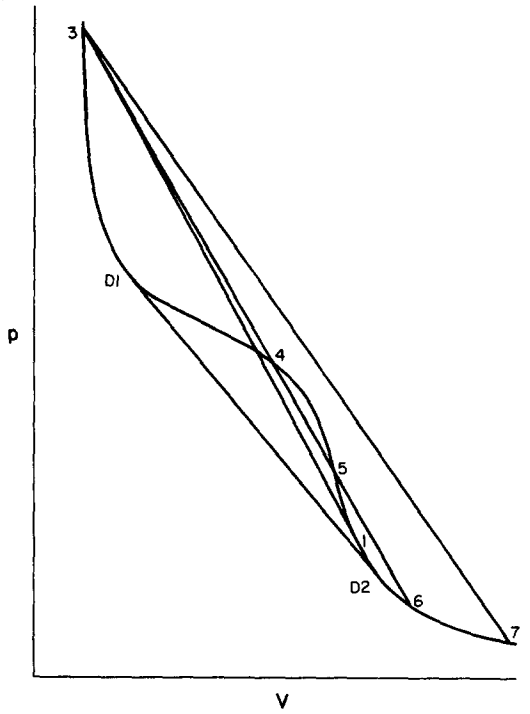

FIG. 5. Interpretation of roots of (20).

where

$$\epsilon_i = \zeta_i - 1,$$

$$B_i = \frac{2}{2+\delta}\left(\frac{1}{3\overline{V}_i} + \frac{\delta}{2} + \frac{\bar{p}_i \overline{V}_i (1+\delta)}{9\bar{a}_i^2}\right), \tag{22}$$

$$C_i = 2/(2+\delta)\{(1 - 3\overline{V}_i + 3\overline{V}_i\delta)/(3\bar{a}_i\overline{V}_i)^2\}.$$

The first root in (21) corresponds to the imposed sonic condition and the second set are the remaining roots. Because we have set $M_i = 1$, the subscript i must now be associated with conditions at the sonic side of the shock.

To make use of these formulas, we specify which side of the shock is sonic, i.e., whether $i = 1$ or 2, the thermodynamic state, $\bar{p}_i$, $\overline{V}_i$, at the sonic state of the shock and the value of δ. Equations (17), (18), (21), and (22) then yield the shock strength as measured by ζ_i. The nondimensional specific volume at the other side of the shock is given by $\overline{V}_i\zeta_i$. The computed values of nondimensional temperature (18) and sound speed (17) may be combined with the sonic condition and (16) to determine A. Equation (13) then yields the pressure at the other side of the shock. This may be written as

$$\bar{p}_{0i} = \bar{p}_i - A\epsilon_i\overline{V}_i. \tag{23}$$

In (23) and all that follows the subscript 0 will denote conditions at the other, nonsonic side of the shock, e.g.,

$$Q_{0i} = \begin{cases} Q_2, & \text{when } i = 1, \\ Q_1, & \text{when } i = 2, \end{cases}$$

where Q is any quantity. Once the thermodynamic state on the nonsonic side of the shock is determined, the temperature, sound speed, and entropy jump may be computed. We have found that the temperature may be written

$$\overline{T}_{0i} = \overline{T}_i(1 + \Delta_i\delta), \tag{24}$$

where

$$\Delta_i \equiv -\frac{3}{8}\frac{\overline{V}_i\epsilon_i}{\overline{T}_i}\left(\bar{p}_i + \frac{3}{\overline{V}_i^2\zeta_i} - A\frac{\epsilon_i\overline{V}_i}{2}\right).$$

The most straightforward derivation of (24) is to combine the equation of state (10) with the momentum equation (13) and the Hugoniot equation (5) to show that $[\overline{T}] = \overline{T}_1\Delta_1\delta = -\overline{T}_2\Delta_2\delta$. It is then a straightforward matter to recast this in the form (24). The sound speed at the nonsonic side of the shock is given by

$$\bar{a}_{0i} = \left(\frac{2}{3}\right)^{1/2}\left(\frac{4\overline{T}_{0i}\overline{V}_i^2\zeta_i^2(1+\delta)}{(3\overline{V}_i\zeta_i - 1)^2} - \frac{1}{\zeta_i\overline{V}_i}\right)^{1/2}, \tag{25}$$

which is seen to be a recast version of (17). The nondimensional entropy jump is found to be

$$\frac{[s]}{c_v} = (-1)^{i+1}\left(\ln(1+\delta\Delta_i) + \delta\ln\left(\frac{3\overline{V}_i\zeta_i - 1}{3\overline{V}_i - 1}\right)\right). \tag{26}$$

The mass equation (3) and definition (8) may be used to show that the Mach number at the other side of the shock may be written

$$M_{0i} = \zeta_i\bar{a}_i/\bar{a}_{0i}. \tag{27}$$

The speed-ordering relation (7) therefore reduces to

$$M_{0i}(-1)^{i+1} \leqslant (-1)^{i+1}, \tag{28}$$

where the equality corresponds to a double sonic shock.

If $\bar{p}_i$, $\overline{V}_i$ are specified at points to the left of D1 in Fig. 5 or to the right of D2, the tangent does not intersect the adiabat and the square root in (21) is not real. When the sonic state is specified between D1 and D2, the tangent intersects the adiabat at two additional points (the only exceptions are the inflection points); these intersections correspond to the $\pm$ signs in (21). In computer solutions both are calculated and both are independently checked against the speed ordering condition (28) and entropy inequality, i.e., (6) combined with (26). As a further independent but unnecessary check, we use the computed values of sound speed and A to compute the Mach number at the sonic side of the shock. Of course, when the computations are correct, this will always turn out to be unity.

Double sonic shocks occur when the square root in (21) becomes zero; i.e.,

$$(B_i - 3)^2 - 12 + 8B_i + 4C_i = 0. \tag{29}$$

This is recognized as the case where the two remaining nonsonic roots, e.g., points 2 and 3 in Fig. 5, also collapse to a double root. The strategy for determining double sonic shocks is to solve (29) for the pressure required to attain the double root. This solution is found to be

$$\bar{p}_i = N_i\{1 + N_i((3\overline{V}_i - 1)/6)\cdot((1+\delta)/(2+\delta))\cdot\overline{V}_i^2\}, \tag{30}$$

where

$$N_i \equiv (3\overline{V}_i(1-\delta) - 2)/(1+\delta)\overline{V}_i^3.$$

We may now choose the specific volume $\overline{V}_i$ at which we desire the double sonic shock. Equation (30) then determines the pressure. Now that the pressure and specific volume are known, we may treat this as a regular sonic shock

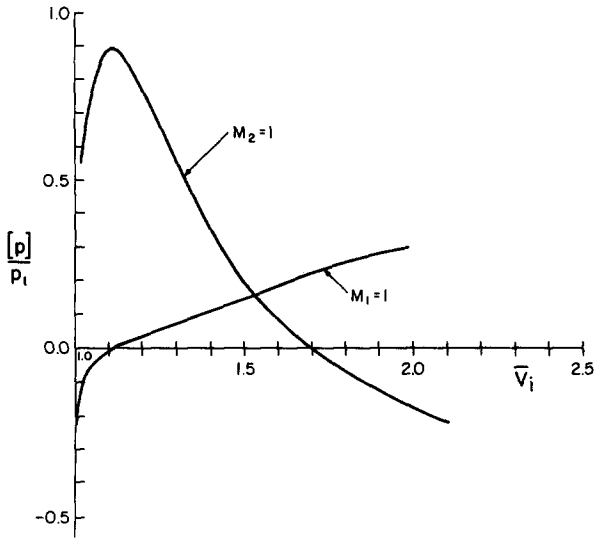

FIG. 6. Variation of sonic shock strength. Both curves correspond to a single shock adiabat. The horizontal coordinate is $\bar{V}_1$ for the $M_1 = 1$ curve and is $\bar{V}_2$ for the $M_2 = 1$ curve.

and make use of (21), (22), etc., to compute the remaining parameters. As in the case of single sonic shocks, the upstream and downstream Mach numbers may be computed and checked once the thermodynamic states and mass flux A are computed.

As an illustration of the use of these formulas we have plotted the variation of shock strength and entropy rise of all sonic shocks possible on a particular shock adiabat in Figs. 6 and 7. The adiabat chosen is that denoted by $\bar{p}^* = 0.826$ in Fig. 3. The double sonic shock for this adiabat has upstream and downstream conditions given by

$$\bar{V}_1 = 1.0062, \quad \bar{p}_1 = 1.0685, \quad \bar{V}_2 = 2.1, \quad \bar{p}_2 = 0.8259,$$

and nondimensional entropy jump $[s]/c_v = 0.34 \times 10^{-4}$.

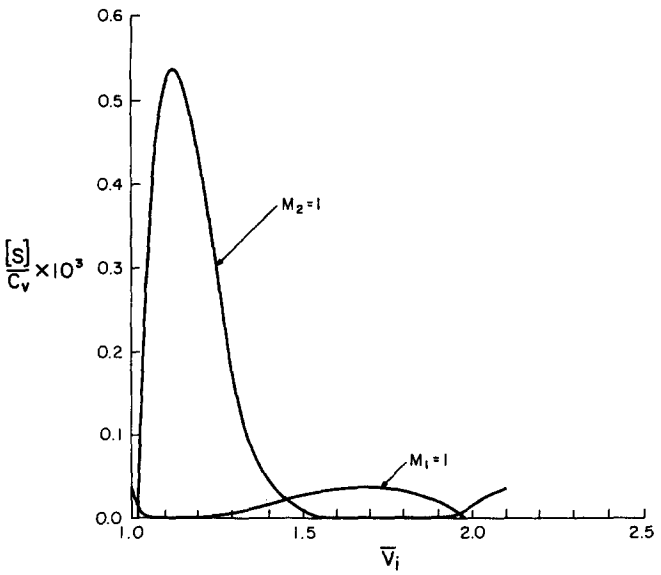

FIG. 7. Variation of entropy rise of sonic shocks. Both curves correspond to a single shock adiabat. The horizontal coordinate is $\bar{V}_1$ for the $M_1 = 1$ curve and is $\bar{V}_2$ for the $M_2 = 1$ curve.

As pointed out above, the sonic state of any sonic shock will always lie between the upstream and downstream states of the double sonic shock. Thus, for the above adiabat we have taken $1.0062 \leqslant \bar{V}_i \leqslant 2.1$. In each figure $\bar{V}_i$ is the specific volume at the sonic side of the shock. Thus, for the $M_1 = 1$ curve, $\bar{V}_i = \bar{V}_1$ with similar remarks for the $M_2 = 1$ curve.

Although the geometrical construction described in the last section suggests that both types of sonic shock are possible over the full range $\bar{V}_i = 1.0062$ to 2.1. However, when the entropy inequality is considered, we find that nonsonic as well as sonic compression shocks in the neighborhood of the double sonic shock violate the entropy inequality; a specific example of a nonsonic shock is found at end of the last section. The points at which the entropy jump changes sign are seen in Fig. 7. For shocks having $M_2 = 1$ the sign change occurs at $\bar{V}_2 \simeq 1.02$ and for shocks having $M_1 = 1$ this occurs at $\bar{V}_1 \simeq 1.98$. Thus, all curves in Figs. 6–7 have been terminated at appropriate points.

The strength of both upstream and downstream sonic shocks goes to zero at the inflection points of the adiabat. The peak in the shock strength of the $M_2 = 1$ curve also roughly corresponds the inflection point. In the $M_1 = 1$ curve there is also a local maximum. In fact, the strength must approach the negative of that of the double sonic shock as $\bar{V}_1$ approaches 2.1. As already discussed and as is seen in Fig. 7, this local maximum will correspond to a negative entropy rise and is not represented here.

IV. SONIC SHOCKS EMBEDDED IN SMOOTH FLOWS

In this section we use our exact solutions to illustrate sonic shocks embedded in smooth flows. The examples chosen correspond to finite amplitude disturbances which evolve from a step function initial condition. That is, all thermodynamic parameters as well as the particle velocity are constant for $x \gtrless 0$; the coordinate system is chosen such that the initial shock position is $x = 0$. To simplify the problem we take all waves to be propagating to the right, i.e., in the positive x direction. This, of course, differs from the classical Riemann problem where the single discontinuity splits into right- and left-moving waves; this more complicated problem will be treated in future studies in the context of shock tubes. To further simplify the problem we take the undisturbed state to be at rest, i.e., $v_r \equiv 0$. Here v is the particle

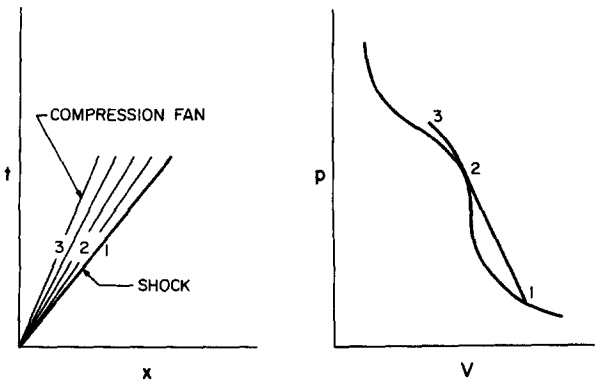

FIG. 8. Example of shock–fan combination. (a) x-t diagram, (b) p-V plane.

velocity and the subscript r refers to conditions evaluated at the undisturbed state. Thus, the subsequent flow will resemble that generated by an impulsively started piston.

When Γ is strictly positive or strictly negative, the initial discontinuity will either spread out into a centered fan or remain intact as a discontinuity propagating to the right. However, in the cases illustrated below the initial discontinuity suffers a partial disintegration into a sonic shock and centered fan or, in the case of a double sonic shock, fans. An example of a compression shock with sonic downstream conditions is sketched in Fig. 8. The flow is taken from state 1 to state 2 through the sonic compression shock and then to state 3 through the isentropic compression fan.

Because the disturbances are taken to be simple waves, the smooth portion of the flow may be computed by the method of characteristics. The exact solution is therefore given by

$$\rho = \text{constant on characteristic lines},$$
$$x = x_0 + \left(v_k + a_k + \int_{\rho_k}^{\rho} \Gamma(r,s_k)\,dr\right)t, \tag{31}$$

where t is the time and the quantity x_0 is the usual integration constant; in centered fans we take $x_0 = 0$. Here the subscript k denotes quantities evaluated at the shock. In the region ahead of the shock we take $k = 1$ and in the region behind the shock we choose $k = 2$. Equation (31) is valid for simple waves in any fluid. For the van der Waals gas discussed here the appropriate expression for Γ is

$$\Gamma = (1/2a\rho^2)\{\rho RTZ/(1-b\rho)^3 - 6a\rho^2\}, \tag{32}$$

where $Z \equiv 2 + 3\delta + \delta^2$. In order to evaluate this on an isentrope, i.e., $s = s_k = \text{constant}$, we must choose the absolute

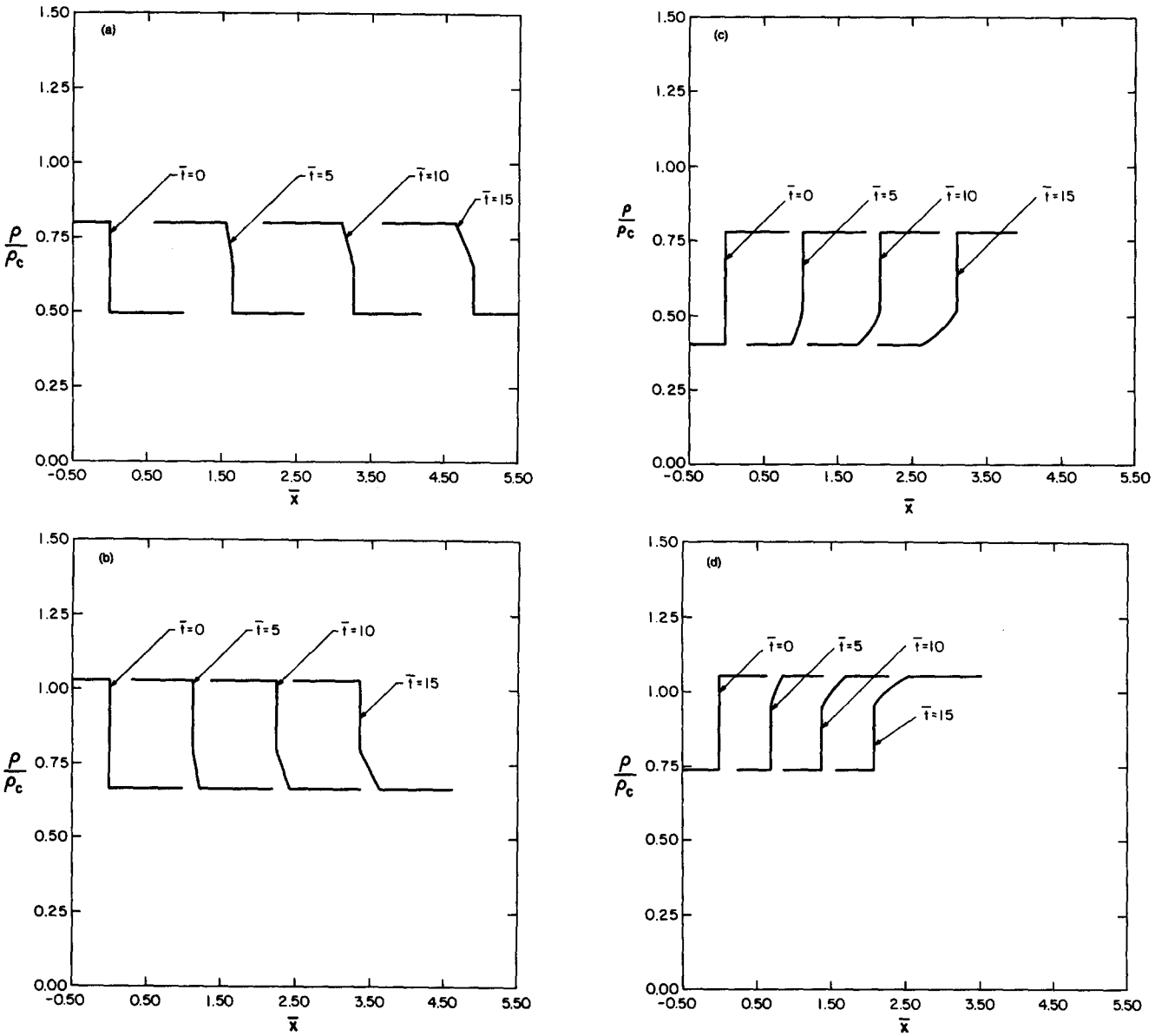

FIG. 9. Computed evolution of a step function initial condition. (a) Compression shock, $M_2 = 1$, (b) compression shock, $M_1 = 1$, (c) expansion shock, $M_2 = 1$, (d) expansion shock, $M_1 = 1$.

temperature according to

$$T = T_k(\{(1-b\rho_k)/(1-b\rho)\}\cdot\rho/\rho_k)^{\delta}, \tag{33}$$

provided $\delta \neq 0$. Results similar to (31)–(33) were employed by Cramer and Sen[10] as part of their analysis of shock formation.

The particle velocities at any point in the flow are given by the simple wave condition

$$v = -a + v_k + a_k + \int_{\rho_k}^{\rho} \Gamma(r,s_k)dr. \tag{34}$$

Because the undisturbed medium was taken to be at rest, the particle speed ahead of the shock v_1 may be computed from (34). If we denote the density, temperature, and sound speed of the undisturbed medium by ρ_r, T_r, and $a_r \equiv a(\rho_r, T_r)$, we find

$$v_1 = a_r - a_1 - \int_{\rho_1}^{\rho_r} \Gamma(r,s_1)dr. \tag{35}$$

In cases where the shock propagates directly into the undisturbed medium, we set $\rho_r = \rho_1$, $T_r = T_1$ which yields the correct result $v_1 = 0$. When a centered fan precedes the shock $\rho_1 \neq \rho_r$, $T_1 \neq T_r$ and, as a result, $v_1 \neq 0$. Once v_1 is determined, the particle velocity downstream of the shock may be computed from the definition of the Mach number (8) with the relative velocity w_k replaced by $u - v_k$, where u is the actual shock speed. Thus, we find

$$M_k = (u - v_k)/a_k, \quad k = 1,2. \tag{36}$$

The solution for v_2 is

$$v_2 = v_1 + M_1 a_1 - M_2 a_2. \tag{37}$$

In the approach taken there, both Mach number and the thermodynamic state on either side of the shock will be known before v_2 is required. In the present study we consider sonic shocks only. Thus, either Mach number, or both, will be identically one in (37). However, there is no advantage to making this specialization at this stage.

Our general method of calculation can be regarded as an inverse approach. The results of Sec. III are first used to compute the sonic shock. The thermodynamic state of the nonsonic side of the shock is set equal to the shock values. For example, in the case depicted in Fig. 8 we would set $\rho_r = \rho_1$, $T_r = T_1$. The density level at the sonic side of the initial step function may be chosen to fix the strength of the centered fan. When this is done, Eqs. (31)–(37) may then be employed to construct a centered fan adjacent to the sonic side of the shock. In the example of Fig. 8 we would simply choose ρ_3 to be some value greater than ρ_2. The velocity distribution may be simultaneously computed through use of (34).

The shock speed may be evaluated by either of conditions (36). As a check on the computations we evaluate u using both formulas. In fact, the shock is plotted by computing the upstream and downstream points

$$\rho = \rho_1, \quad x = (M_1 a_1 + v_1)t,$$

$$\rho = \rho_2, \quad x = (M_2 a_2 + v_2)t.$$

The plotting routine automatically connects these points with a straight line. Correct solutions will always yield a vertical line in ρ-x plots.

TABLE I. Numerical data for Figs. 9 and 10. The quantities ρ_l and ρ_r are the densities to the left and right of the initial discontinuity.

Case	$\frac{\rho_r}{\rho_c}$	$\frac{\rho_l}{\rho_c}$	$\frac{\rho_1}{\rho_c}$	$\frac{\rho_2}{\rho_c}$	$\frac{p_1}{p_c}$	$\frac{p_2}{p_c}$	M_1	M_2	$\frac{[s]}{R}$ $\times 10^4$
Fig. 9(a)	0.497	0.800	0.497	0.645	0.845	0.955	1.019	1.000	0.66
Fig. 9(b)	0.667	1.032	0.801	1.032	1.022	1.077	1.000	0.876	0.97
Fig. 9(c)	0.776	0.400	0.776	0.517	1.013	0.863	1.059	1.000	2.89
Fig. 9(d)	1.053	0.737	0.952	0.737	1.059	0.999	1.000	0.953	0.87
Fig. 10	1.200	0.300	0.994	0.476	1.069	0.826	1.000	1.000	16.94

Computed results for four typical cases leading to sonic shock have been depicted in Fig. 9. The corresponding flow parameters are listed in Table I. The evolution of a double sonic shock has been depicted in Fig. 10. For purposes of comparison we have chosen these such that they lie on the same shock adiabat as used in Figs. 6 and 7. Although there is no natural length or time scale in this problem, the dimensional position x and time t have been scaled with an artificial length L so that

$$x = L\bar{x}, \quad t = L(b/\alpha)^{1/2}\bar{t}.$$

An alternate approach is to cast these results in terms of a similarity variable proportional to x/t. However, we felt the present approach gives a more natural representation of the partial disintegration of the shock as well as the relative speeds involved. Furthermore, in more complex flows containing these as a local element, a length scale will typically be available.

It is useful to relate these shocks to the adiabats sketched in Fig. 4. The compression shocks in Figs. 9(a) and 9(b) correspond to sonic shocks C1–CS2 and CS1–C4 of Fig. 4(a), respectively. The expansion shocks in Figs. 9(c) and 9(d) correspond to the sonic shocks E1–ES2 and ES1–E3 of Fig. 4(b), respectively. Of course, the double sonic shock of Fig. 10 corresponds to D1–D2 of Fig. 4(b).

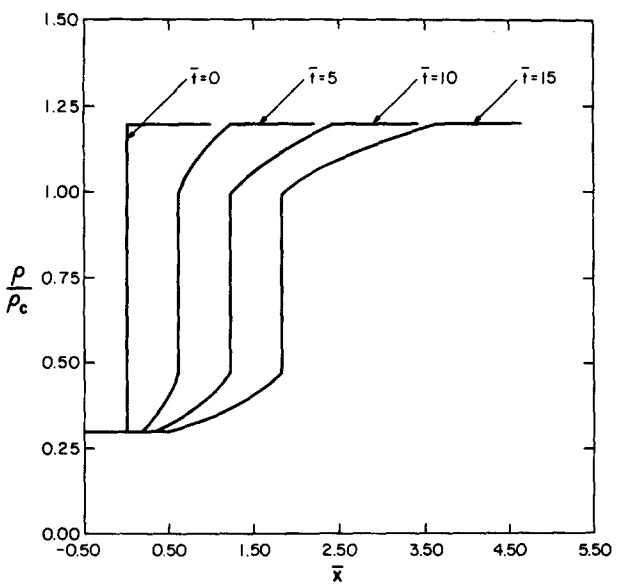

FIG. 10. Computed evolution of a double sonic shock.

V. SUMMARY

The main goal of the present study is to present exact solutions for single and double sonic shocks in van der Waals gases. The key result for single sonic shocks is contained in Eqs. (21)–(22). These are obtained by deriving exact solutions to the shock adiabat (12) or (20). The formulas for Mach number (27) and (28) and entropy rise (26) may be used to eliminate unacceptable sonic shocks. Double sonic shocks are computed through use of the relatively simple result (30). In each case the formulas are explicit and in closed form and therefore have clear advantages over implicit formulations. We expect these will find a number of applications in studies of the inviscid and dissipative dynamics of fluids of type discussed by Bethe[1] and others,[2,5,7–10] i.e., those having embedded regions of negative nonlinearity.

Examples of the application of these formulas in the context of unsteady flows have been provided in Sec. IV. In agreement with weak shock theory[8,9] we find that we may construct sonic shocks which not only satisfy the local conditions (6) and (7) but which are also consistent with some global flow, at least for the cases shown.

[1]See National Technical Information Service Document No. PB 032189 (Office of Scientific Research and Development Rep. No. 545). Copies are available at the U. S. Library of Congress under the NTIS number.
[2]Ya B. Zel'dovich, Zh. Eksp. Teor. Fiz. **4**, 363 (1946).
[3]A. H. Shapiro, *The Dynamics and Thermodynamics of Compressible Fluid Flow* (Wiley, New York, 1953).
[4]L. D. Landau and E. M. Lifshitz, *Fluid Mechanics* (Addison–Wesley, Reading, Mass., 1959).
[5]P. A. Thompson, Phys. Fluids **14**, 1843 (1971).
[6]P. A. Thompson, *Compressible-Fluid Dynamics* (McGraw-Hill, New York, 1972).
[7]P. A. Thompson and K. C. Lambrakis, J. Fluid Mech. **60**, 187 (1973).
[8]M. S. Cramer and A. Kluwick, J. Fluid Mech. **142**, 9 (1984).
[9]M. S. Cramer, A. Kluwick, L. T. Watson, and W. Pelz, J. Fluid Mech. **169**, 323 (1986).
[10]M. S. Cramer and R. Sen, Phys. Fluids **29**, 2181 (1986).
[11]P. Germain, Adv. Appl. Mech. **12**, 131 (1972).